

UDC: 004.93

DOI: 10.15587/1729-4061.2024.311602

# DETERMINING THE EFFECTIVENESS OF USING THREE-DIMENSIONAL PRINTING TO TRAIN COMPUTER VISION SYSTEMS FOR LANDMINE DETECTION

**Oleksandr Kunichik**

*Corresponding author*

PhD Student\*

E-mail: ao669517126@gmail.com

**Vasyl Tereshchenko**

Doctor of Physical and Mathematical Sciences\*

\*Department of Mathematical Informatics

Taras Shevchenko National University of Kyiv

Volodymyrska str., 60, Kyiv, Ukraine, 01033

*The object of this study is the effectiveness of using three-dimensional printing to train computer vision models for landmine detection. The ongoing war in Ukraine has resulted in significant landmine contamination, particularly after Russia's full-scale invasion in 2022. Given the enormous amount of potentially landmine-contaminated land, fast and efficient demining techniques are required, as human probing and metal detectors are labor-intensive and slow-moving. Machine learning offers promising solutions to speed up the landmine detection process by deploying recognition models on robots and unmanned aerial vehicles. However, training such systems faces certain challenges. Firstly, the number of annotated data available for training is limited, which can hinder the model's ability to generalize to real-world scenarios. Secondly, the use of real or even defused landmines is dangerous due to the potential for accidental detonation.*

*This study aims to overcome the problem of limited data and the risk of using real landmines. Three-dimensional printing makes it possible to create safe and diverse training data, which is essential for model performance. The model trained on replicas, achieved 98 % and 91 % precision on printed and actual landmines, respectively. This high precision is attributed to the realism of copies and the use of advanced machine learning algorithms. This approach successfully addressed the research problem due to the safety, accessibility and diversity of copies. The models trained on copies of landmines could be used in humanitarian demining operations. These operations often employ unmanned aerial vehicles or robots to identify landmines that are thrown remotely, exposed on the surface, or partially hidden*

*Keywords: landmine detection, humanitarian demining, demining, unexploded ordnance, explosive remnants of war, landmine clearance*

Received date 02.07.2024

Accepted date 13.09.2024

Published date 25.10.2024

**How to Cite:** Kunichik, O., Tereshchenko, V. (2024). Determining the effectiveness of using three-dimensional printing to train computer vision systems for landmine detection. *Eastern-European Journal of Enterprise Technologies*, 5 (1 (131)), 17–29. <https://doi.org/10.15587/1729-4061.2024.311602>

## 1. Introduction

Landmines continue to pose a significant threat to civilians not only during armed conflicts, but also for decades afterward. They cause thousands of casualties and have a lasting impact on society long after hostilities have ceased. Thus, according to the Landmine Monitor, 608 people were injured by explosives in Ukraine in 2022. After Russia's full-scale invasion, the number of civilian casualties from landmines increased tenfold compared to 2021 (58 casualties) [1]. A particular concern is the risk to children who might be drawn to these dangerous objects due to their often deceptively harmless appearance. The detection and clearance of landmines is an extremely important process for the revival of war-torn regions. The destructive impact of landmines also affects agriculture and infrastructure, rendering large areas of land unsafe for use.

Existing methods for detecting landmines are diverse but often have limitations. Metal detectors and manual probing are labor-intensive and dangerous methods of demining. While promising, cutting-edge technologies like infrared imaging and ground-penetrating radar (GPR) can be costly and produce false positives. Canine units have limitations due to factors such as fatigue and environmental considerations and require a great deal of training.

Computer vision can significantly speed up and make the landmine detection process safer. Recognition algorithms can be applied not only to regular images, but also to GPR and infrared images. It is also worth highlighting that some landmines are plastic, posing a challenge for traditional demining methods such as metal detection, but detectable with computer vision. A significant obstacle to building machine learning models is the lack of data available for algorithmic training and testing. Obtaining real landmine data to train models involves ethical and security concerns. Even defused landmines may be hazardous and obtaining real samples for research is a dangerous process [2].

Given the hazardous nature of handling real landmines and the lack of data to train machine learning models, there is a need to find alternative research approaches. Using 3D printed landmine models enables safe experimentation and diverse data collection. Furthermore, landmines may be resized or modified via 3D printing technology, which also makes it possible to create more durable and adaptable testing models. With the development of 3D printing being used to create landmines for UAV drops, training models on printed copies can also help with detection of improvised explosive devices. (Fig. 1).

Thus, research on the effectiveness of using 3D printed copies to develop methods for detecting landmines is relevant

and has significant potential to improve safety and accelerate the demining process in Ukraine.



Fig. 1. Printed combat landmines: in the central part of the landmine is an explosive substance, the interlayer between the outer casing is filled with bolts as fragments

## 2. Literature review and problem statement

Convolutional neural networks and other machine learning approaches have been the subject of several studies. Convolutional neural networks (CNN) are a type of artificial neural network that specialize in processing images and other data with spatial structure, using convolutional layers to detect local features. Paper [3] uses CNN to recognize landmines from magnetometer images. The above research results show the high accuracy of landmine detection from UAVs. The system was trained on an artificial dataset. Additionally, it was not tested on real data, so it is unclear whether it can be applied in real life. The authors rely on generated images, highlighting the security issues associated with data collection and the lack of publicly available data. Another drawback is the inability to recognize plastic landmines using the system presented in the study. In other words, the paper does not fulfill the fundamental requirement of having good quality data for the study, but instead uses the empirical observation that the generated data is close to the real thing. Additionally, the system has not been tested on real data.

Using machine learning algorithms on GPR pictures is a common method of landmine detection. GPR operates by using a ground-based antenna to send short electromagnetic wave pulses into the soil. The waves are reflected back when they encounter an underground object. An image or profile of subterranean structures can be obtained by examining these return signals. GPR is used in many recent studies for more precise and effective detection. In [4], GPR data was analyzed using CNN, achieving over 93 % precision in the detection of buried objects, including landmines. However, there is still a problem with the system's actual use in landmine detection. The reason for this may be the nature of the study – it was conducted in a laboratory, and it is not clear

how the approaches proposed by the authors will work in real life. However, the methodology was not tested on landmines in real conditions, in different types of soil.

Study [5] conducted in Ukraine used CNN to classify explosive objects, achieving a precision of 97.8 %. However, the study was theoretical in nature and used data from previous work [4], including a dataset.

Article [6] provides a comprehensive overview of machine and deep learning algorithms used in GPR data processing. The authors emphasize the importance of the problem of limited data for training. The main drawback of the study is the absence of any prospects for overcoming the problem of limited data. The authors believe that the creation of synthetic images together with augmentation methods can solve the problem. However, this is only an assumption, and no research has been conducted in this area.

The study [7] proposes a pipeline based on an artificial neural network for detecting buried landmines, which allows to achieve 95 % detection precision. In this study, 9 objects were used to acquire GPR images, but the process of testing and setting up the experiment is cumbersome, so no real application is evident from the study. The data for the study was generated using gpr-max software [8], which allows creating GPR images. The authors plan further experiments with antennas, but as in [6], it is unclear whether the images generated by gpr-max can be used in real-world conditions.

Study [9] demonstrates the potential of using GPR in combination with CNN to detect underground objects. The results of the research demonstrate that it is possible to find improvised explosive devices buried under a road. The main drawback of the study is the insufficient amount of test data. Extending the dataset may improve the research and get it closer to practical implementation.

In [10], a robotic platform is used to detect landmines. The results of the study indicate that it is possible to detect landmines using GPR, but the complexity of the experiment calls into question the practical application of the system. The main problems are the limited dataset (only two types of landmines) and the lack of verification on an independent dataset, which raises questions about its applicability in real conditions.

The problem of limited data can be partially overcome by augmentation. A study [11] showed that data augmentation methods increase the efficiency of deep learning models for landmine detection, reaching 97.4 % precision and 92.6 % recall. The main drawback of the study is the small amount of data collected from the internet. Such a dataset does not have a large variety of data, so more images need to be added to solve this problem.

Other recent studies also examine different methods of landmine detection, for example, [12] examines the use of UAVs with multispectral and thermal sensors. The main drawback of the study is that only one type of landmine is investigated, the dataset has a small number of images (165 images taken from 6 orthophotos), and few types of environments are used. A way to overcome these difficulties could be to increase the data in the dataset, as well as to create more diverse testing conditions.

In [13], landmine installation patterns are analyzed. The possibility of detecting landmines based on a map with other detected ones nearby is studied, for which an artificial dataset with patterns is generated. However, the problems of applying this method in practice remain unresolved, as there is no single rule for laying landmines – they are set depending on the terrain, situation and problem to be solved. As in previous works, artificially generated data does not provide grounds for the practical application of the results of the work.

Study [14] analyzes modern demining methods. It is shown that there is a wide range of methods for landmine detection, but the study does not address the problem of insufficient data for experiments. Also, the issues of practical application of the studied methods remain unresolved. The reason for this may be the slow speed and complexity of setting up the landmine detection systems considered in the study, as they were all conducted in laboratory conditions with a small amount of experimental data.

To summarize, most landmine detection studies have been affected by a lack of data. Many surveys have resorted to creating synthetic imagery [3, 7, 13], using small datasets [6, 10, 12], or even reusing datasets from other studies [5]. Alternatively, 3D computer modeling can be used to overcome the problem of insufficient data, as in the study of car traffic [15], but such data suffers from a lack of realism. Augmentation can also be used, which was studied in [11], but generating images or increasing the amount of data in the dataset does not solve the problem of lack of diverse data.

All of this suggests that it is advisable to conduct a study to identify methods to overcome the problem of limited data for training machine learning systems. An analysis of the literature shows that this is a key obstacle to the development of effective detection systems. Therefore, research aimed at addressing this issue by using 3D printed landmine replicas to generate data for model training is appropriate. Additionally, this approach would make the testing process completely safe, eliminating the possibility of accidental explosion of the experimental material.

---

### 3. The aim and objectives of the study

---

The aim of the study is to determine the effectiveness of using 3D printed landmine replicas for training computer vision models to overcome the problem of data scarcity. This will make it possible to develop a methodology for obtaining machine learning models based on 3D printed copies. The resulting models can be used to identify real landmines, with applications in UAV-based or robotic detection systems.

To achieve this goal, the following objectives were set:

- to develop a dataset for training computer vision models, including images of 3D printed copies of the most common anti-personnel landmines in Ukraine, obtained in different weather conditions (clear, cloudy, rain, snow);
- to train and optimise YOLOv8 computer vision models on the created dataset by increasing the number of images, applying augmentation methods, adjusting hyperparameters;
- to evaluate the effectiveness of the trained models on real landmine images from a separate dataset obtained from professionals.

---

### 4. The study materials and methods

---

#### 4.1. Object and main hypothesis of the study

The object of the study is the effectiveness of using 3D printed landmine replicas to train computer vision models for landmine detection.

The main hypotheses of the study:

- 1) 3D printed replicas can be used to train computer vision models that are effective for landmine detection in real-world conditions;

- 2) models initially trained on 3D printed replicas can be further refined using real-world data through techniques such as adding new data to the dataset, increasing the number of training epochs, and adjusting model hyperparameters.

Assumptions made in this paper:

- 3D printed replicas reproduce the shape, texture and visual characteristics of real landmines in a realistic manner;
- a variety of survey conditions (lighting, background, angle) for 3D printed copies will provide sufficient data variability for effective model training.

Simplifications used in the work:

- some landmine models were scaled down for printing, which may slightly affect the detection precision;
- only visual data (images) were used to train the models, without considering other characteristics (e.g. magnetic properties);
- the results may be worse for metal landmines than if the landmines were printed using metal (due to the lack of metallic shine and texture);
- the study uses images taken in different weather conditions, from different angles. However, this does not cover all possible variations. Recognition efficiency may increase with a larger and more diverse dataset.

As part of the research, some of the landmines commonly used in Ukraine were printed, and a dataset consisting of images of landmine replicas was created. These copies were used to train a computer vision model, using their different appearances and conditions to reflect real-world scenarios.

#### 4.2. Rationale for choosing landmines

Russian forces are using at least 13 types of anti-personnel mines in the war in Ukraine. They are laid on the ground, sometimes camouflaged, but in many cases, the landmines can be seen at least partially. It is because of their widespread presence, surface placement and danger to civilians that the following types of landmines were selected for this study: PMN, PMN-2, OZM-72, MON-50, PFM-1 [16]. It should be added that all anti-personnel landmines are prohibited by international agreements, such as the Ottawa Convention [17].

#### 4.3. Characteristics of selected landmines

Among the many explosive remnants found in the war-affected areas of Ukraine, the following landmines are particularly common and pose a significant threat to human safety:

- PMN: this landmine is commonly known as a "Widow" (Fig. 2, *a*) due to its high trinitrotoluene content (200 grams), which usually results in fatalities when detonated;
- PMN-2: although it contains half the amount of trinitrotoluene as the PMN, this landmine (Fig. 2, *b*) is widely used and produced in various countries;
- OZM-72: this landmine (Fig. 2, *c*), often referred to as the "Jumping Witch" or "Frog". After the activation, the OZM-72 jumps to a height of 60–80 cm, detonating at body level, which increases the potential damage to anyone nearby;
- MON-50: with its unique design (Fig. 3, *a*), this landmine is often hidden under grass or trees. The landmine has a large radius of damage (50 meters);
- PFM-1 (Fig. 3, *b*): very common, usually affecting the feet or hands. Scattered from helicopters or rockets, this landmine can cover large areas, including tree canopy, shrubbery, roofs or building facades. The different colours of the landmine can attract the attention of children.

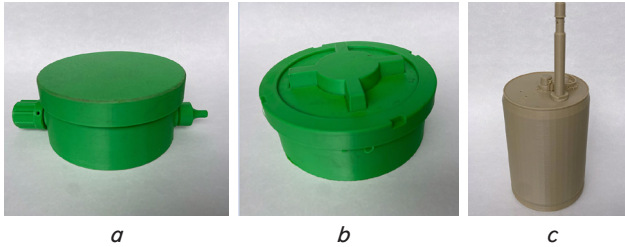


Fig. 2. Printed landmines: *a* – PMN; *b* – PMN-2; *c* – OZM-72

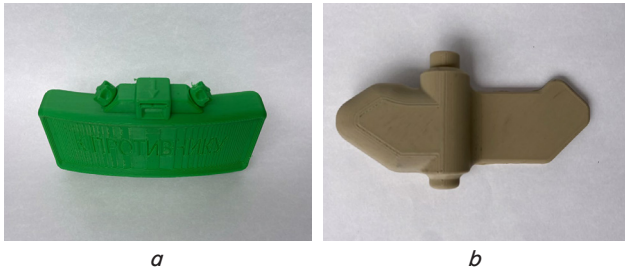


Fig. 3. Printed landmines: *a* – MON-50; *b* – PFM-1

**4. 4. 3D printing process and tools**

3D printing technology allows to produce detailed replicas of selected landmines, which facilitates research. The following process and tools were used for this study:

Software:

- Blender (The Netherlands) [18]: an open-source software for creating 3D models, Blender was used to design and modify 3D models of the selected landmines;

- GIMP (USA) [19]: this free and open-source graphics editor was used for post-processing and fine-tuning of the images of the landmine models.

Equipment: the Prusa i3 MK3S+ (Czech Republic) [20] 3D printer was chosen for its accuracy, reliability and ability to reproduce complex components. This printer also comes with all the necessary software.

Printing specifications:

- infill: the models were printed with a minimum infill of 5–10 %, but this did not affect their strength;

- size adjustment: some models, such as the OZM-72 and MON-50, were reduced to better fit the printing capabilities. The assumption that the quality of recognition would not be affected by the scale reduction was tested on these landmines.

Table 1 lists the publicly available models that were used as a basis for the study.

Table 1 specifies the authors, the license as well as the percentage of infill when printing the model.

Examples of printed models

ID	Qty	Color	Infill	License	Author	Source
PMN	1	Green	5 %	CC BY-NC-ND	mussy	[21]
PMN-2	2	Green	5 %	CC BY, BY-NC-SA	Håkon Benjaminsen, Jonathan Lavoie	[22, 23]
OZM-72	1	Gray	5 %	CC Attribution	valterjherson1	[24]
MON-50	1	Green	5 %	CC BY-NC-ND	mussy	[25]
PFM-1	3	Gray	15 %	CC BY-NC-ND	mussy	[26]

**4. 5. The dataset**

The dataset consisting of 1438 images (Fig. 4) covers a wide range of environments such as sunny day, cloudy day, morning, evening, rain, fog, snow, etc. This study involved the creation of a dataset for five different types of landmines (PMN, PMN-2, OZM-72, MON-50 and PFM-1) taken under different conditions to reflect potential real-world scenarios.

Key details of the photo collection process include:

- the images were taken using a camera with a 64-mega-pixel matrix. Standard settings included ISO 50, 24 mm, F1.8, and shutter speed of 1/60. Various resolutions were used (3468×4624, 3000×4000, 3456×3456), with a standard square resolution of 3456×3456;

- the initial image resolution was standardized to 640×640 pixels. The final model was then trained on both 640×640 and higher resolution images of 1280×1280 pixels for testing on real landmines;

- the images were taken in natural landscapes, near water bodies, under different lighting conditions, among distracting factors (apples, garbage, etc.), in foliage, grass, near buildings, etc.;

- black and white images were added to reduce the impact of color variations, as landmines can come in a variety of colors and shades.

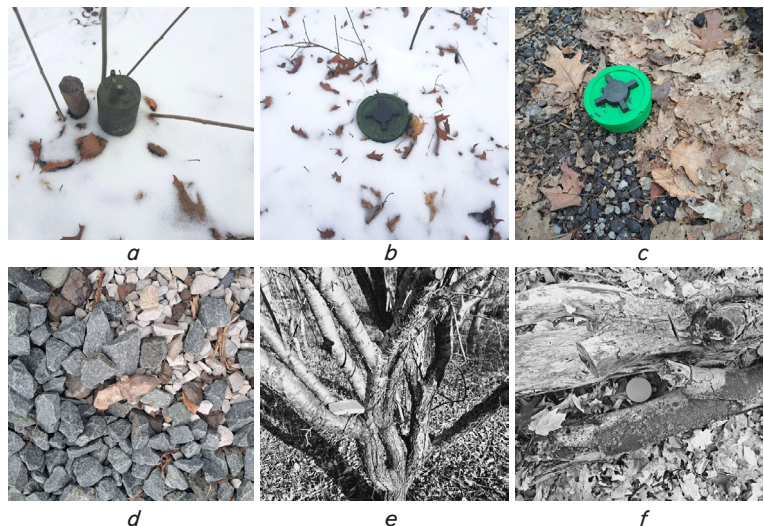


Fig. 4. Examples of images from the dataset: *a* – OZM-72 on snow; *b* – PMN-2 on snow; *c* – PMN-2 on leaves on asphalt; *d* – PFM-1, painted to match the tone of the stones; *e* – MON-50 on a tree (common installation) in black and white; *f* – black and white image of a PMN landmine nestled amongst foliage near a fallen tree trunk

**4. 6. Image annotation and data processing**

The collected images underwent the process of annotation (marking landmines on the image). Several platforms were considered for creating annotations.

Table 1

Comparison of platforms' capabilities for generating landmine detection datasets:

- LabelImg is a simple and free tool, ideal for small projects or the initial stage of annotation. However, it has limited capabilities and does not support automation;

- CVAT is a powerful tool with extensive functionality, including automatic annotation and tracking of moving objects, making it suitable for large projects and landmine video annotation. However, the annotation process is not easy due to the complex interface;

- makesense.ai is an online tool for marking up datasets. It offers an intuitive interface and support for different types of annotations, making it convenient for medium-sized projects. However, it does not save the results of work;

- TORAS (Toronto Annotation Suite) is a web-based image annotation platform. It combines tools for interactive segmentation and also integrates modern artificial intelligence models, such as SAM (Segment Anything Model), to speed up the annotation process;

- Roboflow is an end-to-end solution that covers the process from image acquisition and annotation to training and deployment of models on devices. Offers Automatic annotation;

- Google Cloud Platform allows to create models and has tools for annotation. However, it provides limited control over the training process, for example, it limits the choice of model, the training process, and the setting of hyperparameters;

- Microsoft Azure allows to create models using pre-trained models, which speeds up the development process. However, it has fewer customization options compared to other platforms, such as a simplified training process and hyperparameter settings;

- Amazon SageMaker provides workflow management and automated annotation. But it requires the use of Amazon Web Services, which can be difficult to use.

None of the platforms fully satisfied the requirements of this study. For example, TORAS has convenient annotation tools, but at the time of the study's launch it had a 1GB data size limit, while the data volume exceeded 3 GB. Roboflow has excellent augmentation tools, but the web interface for annotation is very slow. Thus, it was decided to annotate in a self-developed program that imported data to Google Cloud Storage, where images were stored in 640×640 and 1280×1280 sizes. Then the images were uploaded to the Roboflow platform, where the augmentations from Table 2 (from the study [11]) were applied to them.

Roboflow augmentations

Augmentation name	Purpose of use
Flip: Horizontal, Vertical	To prevent memorizing the positions of objects
90° Rotate: Clockwise, Counter-Clockwise, Upside Down	To prevent memorizing the positions of objects
Grayscale: Apply to 45 % of images	To address varying object scales and challenging recognition conditions
Noise: Up to 5 % pixels	To address occlusion of small objects
Mosaic	To enhance data variety via combining

Table 2 explains the purpose of each augmentation technique in the "Purpose of use" column.

#### 4.7. Model training

To fully control the process, the training was performed on a Tesla T4 GPU with 15102 MiB available in the Google Colab service. At this stage, the YOLOv8 algorithm is used, in which augmentations from Table 3 are additionally applied.

Table 3 shows all possible augmentations of YOLOv8, including those that were not used in this study. The characteristic of the value type is given in parentheses – percentage, fraction, degree (+/- degree means that the value can be negative).

Table 3

YOLOv8 augmentations (0.0 – not applied)

Key	Value	Description
hsv_h	0.015	Image HSV-Hue augmentation (fraction)
hsv_s	0.7	Image HSV-Saturation augmentation (fraction)
hsv_v	0.4	Image HSV-Value augmentation (fraction)
degrees	0.0	Image rotation (+/- degree)
translate	0.1	Image translation (+/- fraction)
scale	0.5	Image scale (+/- gain)
shear	0.0	Image shear (+/- degree)
perspective	0.0	Image perspective (+/- fraction), range 0 – 0.001
flipud	0.0	Flip image up-down (probability)
fliplr	0.5	Flip image left-right (probability)
mosaic	1.0	Image mosaic (probability)
mixup	0.0	Image mixup (probability)
copy_paste	0.0	Copying part of images one to one (probability)

#### 4.8. Model selection rationale

Computer vision landmine detection is a complex task that requires great precision and reliability. To determine if the current computer vision models for object detection are appropriate for landmine detection, a review of these models was conducted out.

Overview of the models:

- R-CNN and its variants (Fast R-CNN, Faster R-CNN, Mask R-CNN): these models operate slowly but can attain great accuracy;

- SSD (Single Shot MultiBox Detector): this model is faster than R-CNN and predicts item positions and classes at the same time. However, its accuracy may be less precise, especially for small items;

- YOLO (You Only Look Once): fast and accurate object detection system. It processes images in a single pass, making it ideal for real-time applications.

*Model selection.*

For this study, the YOLOv8 model was chosen because it has several advantages that make it particularly suitable for landmine detection:

- high accuracy: YOLOv8 demonstrates high object detection accuracy, which is critical for landmine detection, where errors can have fatal consequences;

- speed: YOLOv8 operates in real time, allowing for fast processing of images from UAVs and other automated systems;

- flexibility: YOLOv8 can be easily adapted to detect different types of objects different shapes and sizes, including landmines.

The YOLO algorithm was introduced in 2015 [27]. The algorithm determines the bounding boxes and associated class probabilities directly from the full images in one pass. The algorithm processes images in real time at 45 frames per second.

A smaller version, Fast YOLO, processes 155 frames per second, achieving twice the average accuracy of other real-time detectors. Despite the higher number of localization errors, YOLO is much less likely to predict false positives where there is nothing. This makes it a reliable choice for applications such as landmine detection. One of the most recent versions, YOLOv8 [28], has been applied in various fields. These include real-time flying object detection [29], tracking people who shoot [30], and high-resolution aerial photography [31]. The algorithm has also shown promise in medical applications, such as brain tumor detection [32] and real-time arrhythmia monitoring [33]. Additionally, it has been used in vehicle security through license plate and face recognition [34].

Once the model was trained, new photographs of the same landmines, but taken in different locations and under different conditions, were used for testing. The goal was to find out if additional images were needed to further improve the model. Additionally, the model was tested on a separate dataset created from images of real landmines obtained from professional deminers. This cross-comparison was intended to assess how well the model learned on replicas and whether it could generalize its learning to real images.

## 5. Results of research on the use of 3D printing to create computer vision models for landmine recognition

### 5.1. Development of a dataset for training computer vision models

After selecting the landmine types and finding their models in the public domain, 3D copies were printed, with multiple copies printed for some. During the experiments, the landmines were painted in different colors, placed at different angles, partially overlapped, and photographed next to other objects.

The process of creating a dataset was carried out iteratively by conducting a series of surveys (100–200 new images each), experiments and model training, including the use of

augmentation methods, evaluation of results, and setting goals for the next iteration. Table 4 summarizes the results of various experiments that show the influence of the number of images, various augmentations, and settings on the performance of the model.

From Table 4, one can see that during the experiments, the performance of the model gradually increased, but the image processing time per second, and, accordingly, the total time also increased.

### 5.2. Model training and optimization, statistical metrics

The YOLOv8 algorithm was trained on a dataset of 1438 photographs. The application of augmentation methods increased the number of images to 3452. These images were divided into training (3021, or 89 %), validation (287, or 8 %), and test (144, or 4 %) sets. In the process of testing, the proposed approaches to augmentation from [11] were modified for a better model performance. The model demonstrated 98.0 % precision and 98.2 % recall, which indicates a positive result of the use of 3D printed models for landmines detection.

The model training process was carried out iteratively, by changing the size of the batch of images processed in one epoch (a full pass through the training dataset) and experimenting with different data augmentation methods. For images of 640×640 pixels, a batch size of 32 was used. However, for higher resolution images (1280×1280), the maximum batch size was reduced to 8 due to limited computing resources, which led to a decrease in the learning speed by about four times (Table 4: pairs of experiments 7 and 7.1, 8 and 9). When testing additional augmentations, such as Mixup and Copy-paste, it was found that they increase precision but decrease model recall (Table 4: Experiments 8 and 8.1). Given the greater importance of recall for the landmine detection task, these augmentations have not been included in the final model. Adding mosaic augmentation, which combines multiple images into one, significantly improved the model's performance, achieving high precision (98.0 %) and recall (98.2 %).

Table 4

Comparison of the results of different experiments

No.	Qty	Size <sup>1</sup>	Precision	Recall	mAP <sup>2</sup>	Speed <sup>3</sup>	Note
1	195	640	74.9	71.2	80.8	2	From [11]: Preprocessing: Auto-Orient, Resize (to 640×640), Auto-Adjust Contrast (Using contrast stretching). Augmentations: Flip (Horizontal, Vertical), Rotate 90° (Clockwise, Counter-Clockwise, Upside Down), Grayscale (30 % of images), Noise (15 % of pixels), Augmentations from Table 3
2	130	640	72.5	64.9	66.7	4	Same as 1
3	250	640	89.4	84.9	94.5	14	Same as 1
3.1	250	640	90.8	84.3	91.5	14	Same as 1, but Grayscale 100 %
4	400	640	74.9	71.2	80.5	20	Same as 1
4.1	400	640	95.0	91.9	93.4	25	As before, but Grayscale increased to 60 % and Noise decreased to 2 %
5	500	640	93.8	89.8	94.1	28	Same as 1
6	500	640	92.9	86.6	92.8	48	Same as 1, but Noise decreased to 5 %
6.1	500	640	95.2	94.6	97.6	48	After a series in the set of experiments as in 6, Shades of gray: 45 %, Mosaic
7	800	640	91.9	88.6	94.1	45	Same as 1
7.1	800	1280	96.5	91.6	96.4	170	Same as 1, but Resize up to 1280×1280
8	1000	640	96.8	96.4	97.8	59	Same as 6.1
8.1	1000	640	97.3	94.8	98.4	65	Same as 6.1, but YOLOv8 Augmentations, Copy-Paste (0.5)
9	1000	1280	98.5	97.7	98.9	240	Same as 6.1, but Resize to 1280×1280
10	1438	640	97.9	96.7	98.7	120	Same as 6.1
11	1438	1280	98.0	98.2	99.3	240	Same as 6.1, but Resize to 1280×1280

Note: <sup>1</sup> – resolution of the side of the square image in pixels; <sup>2</sup> – mAP: mean average precision (4); <sup>3</sup> – average image processing speed per second.

To evaluate the performance of the model, this work uses such metrics as precision and recall. Additionally, the paper presents metrics based on the concept of Average Precision (AP).

Precision (1) measures the ability of the model to correctly identify landmines among all detected ones and is calculated according to the following formula (1):

$$\text{Precision} = \frac{\text{True Positives}}{\text{True Positives} + \text{False Positives}}, \quad (1)$$

where True Positives are the number of correctly detected landmines, False Positives are the number of falsely detected landmines. High precision means that the model minimizes the number of false positives (the proportion of falsely detected landmines is minimal), which is very important in the context of landmine detection, where false detections can waste demining resources.

Recall (2) measures the ability of the model to detect all relevant cases of landmines in the dataset and uses False Negatives instead of False Positives – the number of undetected landmines:

$$\text{Recall} = \frac{\text{True Positives}}{\text{True Positives} + \text{False Negatives}}. \quad (2)$$

High recall means that the model can find the majority of landmines, which is critical in the landmine detection process.

The choice of precision and recall for evaluating the performance of the landmine detection model is determined by the specificity of the task, where:

- False Positives are undesirable but less critical than False Negatives. False detection will lead to additional checks and is time-consuming, but will not endanger life. On the other hand, not detecting a landmine is undesirable;

- the balance between precision and recall is important. An ideal model would have high values for both metrics. In practice, however, it is often necessary to find a compromise between the two, tuning the model in such a way as to minimize the risks associated with false negatives while maintaining an acceptable level of false positives.

Precision and recall are more clearly characterized using a confusion matrix (Fig. 5).

		Positive	Negative	
Actual	Positive	True Positive	False Positive	Predicted
	Negative	False Negative	True Negative	

Fig. 5. Confusion matrix for binary classification:

**True Positives** – the number of objects of the positive class that the model correctly classified as positive;  
**False Positives** – the number of objects of the negative class, which the model incorrectly classified as positive;  
**False Negatives** – the number of objects of the positive class, which the model incorrectly classified as negative;  
**True Negatives** – the number of objects of the negative class that the model correctly classified as negative

Explanation:

- a confusion matrix is a table that shows how the model classifies objects. It has two axes: one axis represents the actual classes of objects, and the other represents the classes predicted by the model;

- in the context of landmine detection, a "positive" class means a landmine, and a "negative" class means no landmine.

Average Precision (3) (AP) is a metric used to measure precision in relation to recall. It is the average precision value calculated for different recall thresholds, usually expressed through the "precision-recall" curve. AP is quantified as the area under this curve, which is calculated by integrating precision over recall over the corresponding interval:

$$AP = \int_0^1 p(r)dr, \quad (3)$$

where  $p$  and  $r$  are precision and recall, which are calculated according to formulas (1) and (2).

Mean Average Precision (mAP) is calculated as follows:

$$mAP = \frac{1}{n} \sum_{k=1}^n AP_k, \quad (4)$$

where  $AP_k$  is the average precision of class  $k$ , where  $k$  is from 1 to  $n$ .

Intersection over Union (5) (IoU), or Jaccard index, measures the ratio of the area of intersection and the area of union of two bounding boxes – the one that outlines the object (Ground-truth), and the one predicted by the model:

$$\text{IoU} = \frac{\text{True Positives}}{\text{True Positives} + \text{False Negatives} + \text{False Positives}}. \quad (5)$$

The closer the value of the coefficient is to one, the closer the predicted frame is to the true boundary.

mAP50 is the value of the mean average precision (4) at an IoU of 0.5 (or 50 %).

mAP50-95 is the value of the mean average precision (4), calculated for different IoU thresholds from 0.5 to 0.95 (or from 50 % to 95 %). This is a more stringent metric than mAP50 because it averages the mAP values over a range of IoU values.

Using both mAP50 and mAP50-95 together provides a deeper understanding of model performance. mAP50 shows that the model generally recognizes the object, but the frame may be inaccurate, while mAP50-95 focuses on the accuracy of object location recognition. This approach makes it possible to compare the results with other studies, as well as to determine directions for improving the model. For example, if a high mAP50 is combined with a low mAP50-95, this indicates the need to improve the detection boundary of the identified landmines.

The above metrics make it possible to evaluate the performance of different models on the same data. It is important to note that model performance can vary significantly across different datasets, so model evaluation should be conducted on data that is as representative as possible of the actual application.

Fig. 6 shows plots demonstrating the change in precision, recall, mAP50, and mAP50-95 during model training over 100 epochs (experiment 8.1, Table 4).

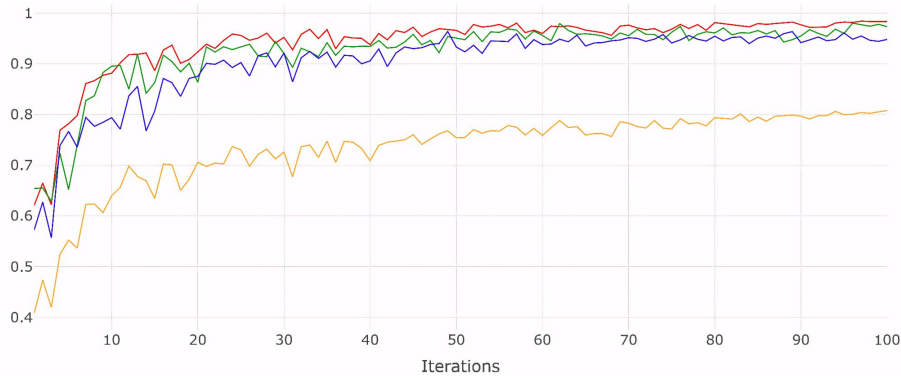


Fig. 6. Plot of changes in precision, recall, mAP50, and mAP50-95 during training over 100 epochs

Another tool for analyzing the model’s performance is the confusion matrix (Fig. 7), which has real values for one of the coordinates, and predicted values on the other. For example, for the first column, of all values, 6 percent were recognized as background, 94 % were recognized correctly.

The normalized confusion matrix (Fig. 7) allows a detailed analysis of the model’s performance and reveals its strengths and weaknesses. As can be seen from the matrix, the model demonstrates high precision for most classes of landmines, especially for MON-50 (100 %, class 14) and PMN-2 (98 %, class 16). However, the model has difficulties in distinguishing the PFM-1 landmine (class 0) and the background, which leads to false positives (6 %). This may be because PFM-1 has a small size and has a variety of colors, which makes it difficult to detect it against the background of the natural environment (see the intersection of the last column and the first row). On the other hand, the model rarely misses landmines, which is confirmed by the high recall for all classes. Even in cases where a landmine is misclassified, it still appears as an object requiring attention (for example, OZM-72 is sometimes categorized as MON-50).

Fig. 8 shows the results of recognition of some printed landmines that have not been included in the dataset for training the model. The model demonstrates high efficiency in detecting printed landmines, which confirms its ability to generalize and recognize key characteristics, such as shape, size and texture.

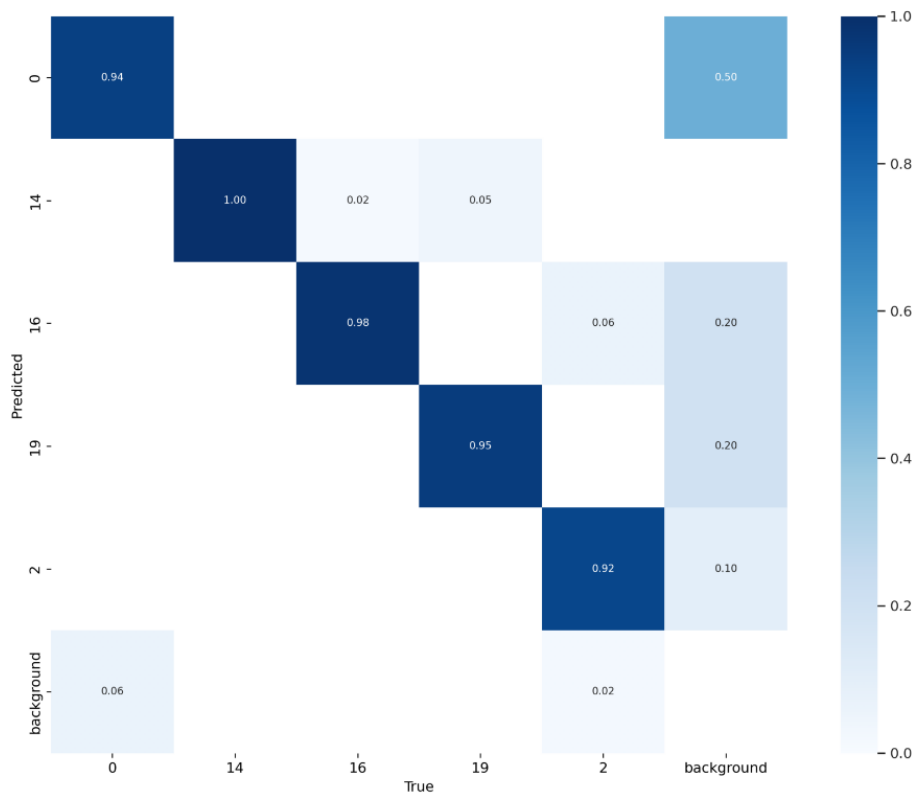


Fig. 7. The normalized confusion matrix for the training dataset of printed landmines: 0 – class for PFM-1; 14 – MON-50; 16 – PMN-2; 19 – OZM-72; 2 – PMN

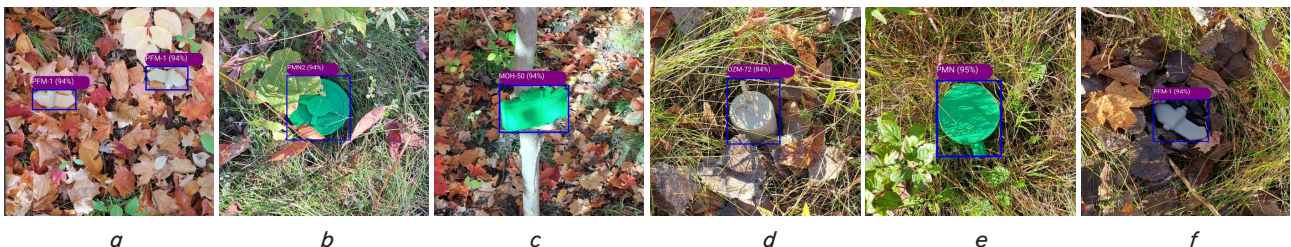


Fig. 8. Examples of successful recognition of 3D printed copies of landmines that have not been included in the training dataset: a – PFM-1 of gray color on the background of foliage; b – PMN-2, partially hidden behind leaves among the grass; c – MON-50 in the sunlight on a tree; d – OZM-72 in the sunlight among leaves and grass; e – PMN in the sun among the grass; f – PFM-1 on the leaves

The images for verification in Fig. 8 are made in such a way as to confuse the model. Percentage values show the recognition probability.

**5. 3. Evaluation of model performance using an independent dataset collected from real landmines**

Fig. 9 shows examples of the model recognizing real landmines, albeit with slightly lower precision compared to 3D printed copies.

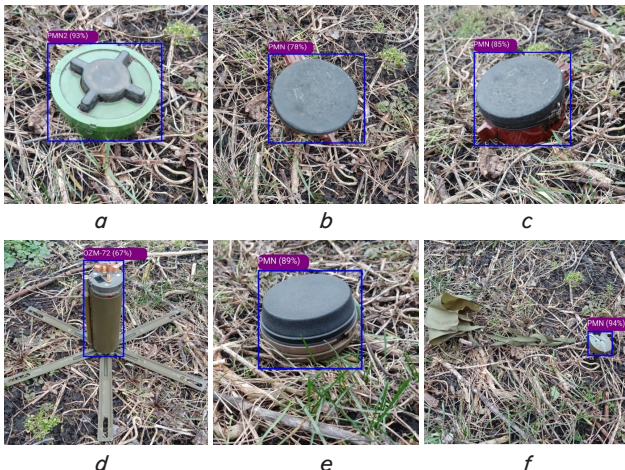


Fig. 9. Examples of recognition on images of real landmines taken by deminers: *a* – accurately recognized PMN-2; *b*, *c* – accurately recognized PMNs; *d* – POM-3, misclassified as OZM-72; *e* – PMN-4, misclassified as PMN; *f* – POM-3 parachute cap, misclassified as PMN

The top row of the figure shows examples of accurate recognition, while the bottom row illustrates cases where landmines were detected but misclassified. The model incorrectly recognized some landmines that had not been included in the training dataset. These landmines were visually similar to the ones the model was trained on.

Table 5 presents the results of testing model from Experiment 11 (Table 4) on data independent of training – printed and real landmines.

From the results, it can be concluded that the model obtained by using 3D printed copies of landmines shows good results, which can be considered as a starting point for further improvement. However, to deploy this model in real-world scenarios, a significantly larger dataset is needed (approximately 5–7 times the size used in this study. For example, for just one type of object, according to Google Cloud Platform recommendations, at least 1,000 images are needed, while training the model requires more than a thousand epochs.

Table 6 presents the statistical indicators for each landmine type in the dataset.

Table 5

Results of model testing with new data

Type of new images	Qty	Precision %	Recall %	mAP50 %	mAP50-95 %
3D printed landmines	402	98.4	98.6	99.1	85.1
Real landmines	254	91.0	79.1	87.5	65.5

Table 6

Results of testing the model on real landmines

ID	Precision %	Recall %	mAP50 %	mAP50-95 %
PFM-1	78.0	84.2	89.1	61.2
MON-50	94.3	60.0	77.1	57.9
PMN-2	93.2	90.5	94.1	73.9
OZM-72	92.4	81.0	87.8	63.4
PMN	97.2	79.5	89.4	71.2
Mean	91.0	79.1	87.5	65.5

Fig. 10 shows the normalized confusion matrix, which corresponds to Table 6.

In the matrix from Fig. 10, it is possible to examine the result of the detection of each of the types of landmines. Attention is drawn to the large number of incorrectly recognized class 14 (MON-50) objects. This may be due to the fact that visually this copy is the least similar to the real landmine. To improve the results, one can add more images of this landmine, design a more realistic model of the landmine, print this model in full size, or try different colors.

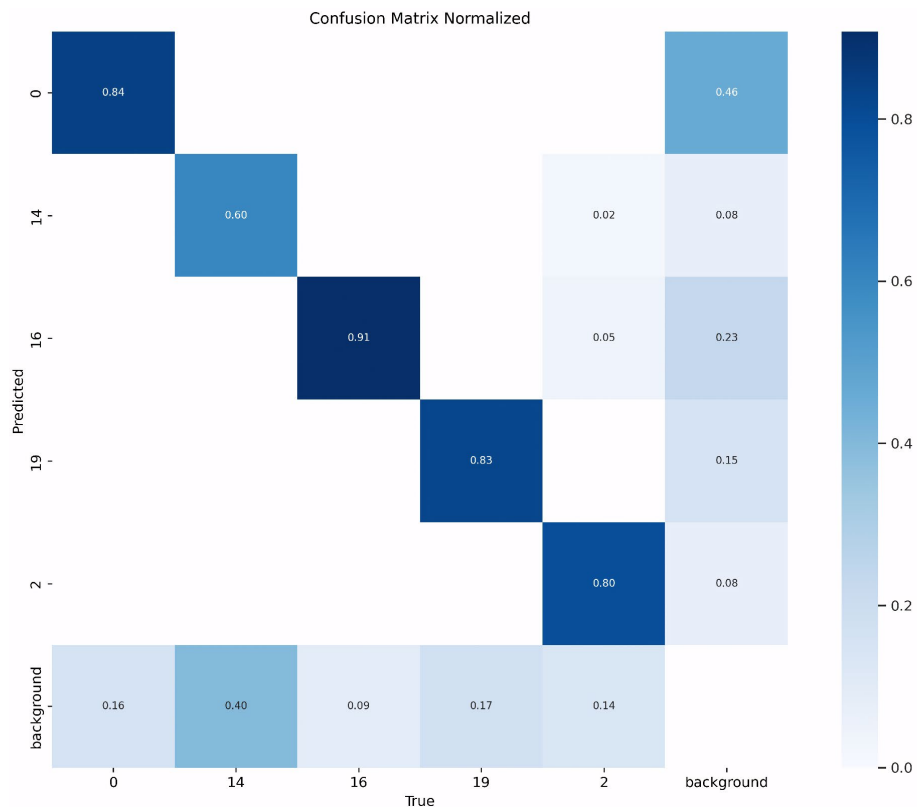


Fig. 10. Normalized confusion matrix for the dataset from real landmines: 0 – class for PFM-1; 14 – MON-50; 16 – PMN-2; 19 – OZM-72; 2 – PMN

## 6. Discussion of the results of the study on the use of 3D printing to create computer vision models for landmine recognition

To create a dataset, 3D models of five types of anti-personnel landmines, the most common in Ukraine, were found (Table 1). Landmine copies were printed on a Prusa i3 MK3S+ 3D printer using PLA plastic with a minimum infill of 5–10 % (Fig. 2, 3). To ensure diversity of data, 1438 photographs were taken under different environmental conditions (clear, cloudy, rain, snow, etc.) and from different angles (Fig. 4). The obtained dataset contains images of landmines in different types of terrain, with different lighting and degree of visibility, which allows training computer vision models on more realistic data.

The YOLOv8 model [28] was chosen to solve the problem of landmine recognition due to its high precision and speed. The created dataset of 3D printed copies of landmines was used to train the model. The learning process was carried out iteratively, with gradual adjustment of the hyperparameters of the model and the use of various methods of data augmentation, in particular those proposed in [11] (Tables 2, 3). As a result, high precision (98.0 %) and recall (98.2 %) were achieved on the test dataset (Table 4), which confirms the effectiveness of using 3D printed models.

For further analysis of the model's performance, testing was conducted on an independent validation dataset from 3D printed landmines, on which the model also demonstrated high performance (Fig. 8, Table 5). This shows that the model is able to generalize and successfully detect landmines in new images.

At the final stage of the research, the obtained model was tested on an independent dataset consisting of 254 images of real landmines (Fig. 9). The test results given in Table 5 showed that the model achieved an average precision of 91.0 % and recall of 79.1 %. These results are attributed to the high similarity of printed landmines to real ones, as well as the high learning and generalization ability of the YOLO algorithm.

However, for some types of landmines, including MON-50 and PMN, precision and recall were lower than for others (Table 6). Note that these results may be due to several factors. Firstly, the images in the training dataset were taken from a greater distance (1–1.6 meters) than the images in the test dataset, which were taken up close. Secondly, the 3D printed copy of the MON-50 landmine did not fully reproduce the complex shape and texture of the real landmine, which could affect the accuracy of its recognition.

The matrix in Fig. 10 shows that the low recall for MON-50 in Table 6 is due to the fact that not all landmines were recognized. Also, for OZM-72 (class 19), the number of unidentified landmines is slightly higher (17 %). Overall, however, the model demonstrated its capability to detect landmines with high accuracy.

This study confirms that 3D printed landmine replicas are an effective tool for data-poor demining research. They are completely safe and allow a wider range of scientists to conduct research and implement new ideas. 3D replicas can serve as an excellent starting point for training machine learning algorithms, which can later be fine-tuned on real data. This opens new opportunities for the development of more effective and affordable landmine detection methods, which is essential for humanitarian demining and the restoration of safety in war-torn areas.

One of the main advantages of this research is the ability to conduct experiments under real conditions. For example, unlike [3, 4], which conducted experiments on a sandy site

with buried landmines, this study conducted experiments in several locations (parks). Furthermore, unlike [5], which utilized the dataset from [4], this study used its own dataset. Another advantage is the variety of landmines used in this research (chosen as the most common in the war in Ukraine), unlike [12], which only used one type, the PFM-1. In contrast to [15], in which to detect landmines from a UAV, the data was transferred to a computer for further processing, in this study the YOLO framework allows for real-time object recognition. Unlike studies [3–5, 7], in which limited or synthetic data were used, this study included testing the model on real landmines, which makes it possible to assess its practical suitability. It is the lack of a large amount of data for analysis, as well as the lack of comparison of results on real landmines, that can lead to the fact that the resulting methodology will not work in real life.

This study demonstrates that when data is scarce, 3D printing can successfully enrich the training and testing datasets for models designed to recognize real landmines. Models trained on printed landmines can be used as a starting point for testing under real conditions. In this case, when testing, it is necessary to find cases when the model incorrectly recognizes the object and add new data to the training process. Studies like [3–5, 7] could potentially achieve better results by incorporating 3D printing for dataset creation. The high performance of the models obtained in this study is attributed to the systematic approach to creating a dataset, the visual similarity of the models to real landmines, and the reliability of modern computer vision algorithms.

Among the limitations in the current study, attention should be paid to the importance of reducing the size of the object. Perhaps the reduced size of the MON-50 model contributed to its lower recognition accuracy. Another potential limitation is the camera distance of 1–2 meters used in data collection. Adapting the model's architecture or exploring alternative computer vision algorithms may be necessary for effective UAV image analysis, as demonstrated in [35] for aircraft recognition.

Another constraint of the study is the limited number of landmine types represented in the dataset. Although the most common types of landmines used in the war in Ukraine were chosen, inclusion of a greater variety of landmines would have allowed for a more versatile model. This task is planned to be solved in the next stage of research aimed at developing a software for detecting a wide range of landmines.

Another drawback is the insufficient realism of some 3D models of landmines, including OZM-72 and MON-50. During the course of the study, many more high-quality models of landmines appeared in volunteer projects that print landmines for the military (training and combat), so it is planned to take them as a basis for future research.

To improve the model, it is possible to investigate the use of more modern feature extraction methods, such as ORB [36] or AKAZE [37], which are more robust to changes in lighting and perspective than the classic SIFT and SURF methods. In addition, the application of other modern neural network architectures could be considered to improve the results. For example, EfficientDet [38] is known for its high accuracy and computational efficiency, which can be especially important when deploying the model on mobile devices or resource-constrained UAVs. Models based on transformers (DETR [39], Deformable DETR [40]) are characterized by high precision on complex data and efficient processing of high-resolution images. This could be useful for detecting landmines in aerial or UAV images. These approaches

could improve the model's ability to discriminate between landmines and background, especially for classes with high mismatches, and provide higher detection accuracy and speed. However, it is worth considering that some of these methods may require more data for training or have a higher computational complexity. To increase the accuracy of detecting real landmines, it is necessary to expand the dataset and improve the realism of 3D models or add more of their varieties. It is also worth investigating the possibility of using additional methods, such as data augmentation and tuning the hyperparameters of the model, to improve its generalizability.

In further research, attention should be focused on the creation of a landmine detection system that can be used under real conditions in Ukraine, as well as in other countries. To achieve this goal, the dataset needs to be expanded to include more types of landmines and images obtained under different conditions. 3D printed models could be used as a starting point, followed by testing on more real-world data with professional deminers. This could improve the precision and generalizability of the model. In addition to using the visual spectrum, it is possible to integrate data from other sensors, such as magnetometers and GPR. This could improve the accuracy of landmine detection, especially those that are difficult to identify by visual features alone. 3D replicas of landmines could be used to collect and analyze data from these sensors. Having achieved some results in the construction of the dataset, it is possible to explore the use of more complex neural network architectures and learning methods, which can improve the precision and speed of landmine detection. Computer vision models obtained in this way could be used in other applied aspects of demining – UAV terrain scanning, robots, etc. Another potential area of application for 3D printed landmine replicas could be to overcome the difficulties associated with remote or camouflaged installations.

---

## 7. Conclusions

---

1. The created dataset containing about 1500 images of 3D printed replicas of landmines in various conditions has demonstrated its effectiveness in training the YOLOv8 model, which achieved high precision and recall. This result confirms that 3D printed replicas could be used to create diverse and representative datasets for training computer vision models. Due to its safety and low cost, this approach could be used both for research purposes and practical applications, for example, for initial training of models or for supplementing datasets with real landmines.

2. Training of the YOLOv8 model on the created dataset of 3D printed copies of landmines, using data augmentation methods, has made it possible to achieve high precision (98.0 %) and recall (98.2 %). These results confirm the effectiveness of using 3D printed replicas to train computer vision models for landmine detection. The high rates of precision and recall are explained both by the quality and diversity of the dataset, and by the efficiency of the YOLOv8

algorithm, as well as the applied augmentation methods. Analysis of the confusion matrix revealed that the model has potential for further improvement, by studying the reasons for recognizing the background as a landmine and by investigating other neural network architectures.

3. Testing the YOLOv8 model on an independent dataset of real landmine images showed that it achieved high precision of 90.1 % and recall of 79.1 %. However, precision and recall varied considerably for different types of landmines. For example, for the PFM-1 the precision was 78 %, while for PMN – 97.2 %. The same applies to recall – from 60 % for MON-50 to 90.5 % for PMN-2. This may be due to the fact that some 3D printed replicas do not fully reproduce the features of real landmines, as well as the limited number of images of real landmines in the testing dataset. This study showed that 3D printed copies of landmines can be effectively used for pre-training computer vision models.

---

### Conflicts of interest

---

The authors declare that they have no conflicts of interest in relation to the current study, including financial, personal, authorship, or any other, that could affect the study, as well as the results reported in this paper.

---

### Funding

---

The study was conducted without financial support.

---

### Data availability

---

The manuscript has associated data in the data warehouse (public datasets on printed and real landmines – <https://universe.roboflow.com/oleksandr-kunichik-sugbr>). The data will be provided upon reasonable request.

---

### Use of artificial intelligence

---

The authors confirm that they did not use artificial intelligence technologies when creating the current work.

---

### Acknowledgments

---

The authors would like to thank Nina Liu of the Toronto Public Library for her invaluable assistance with the 3D printing technique, as well as Forester and S.T.A.L.K.E.R., whose valuable advice, photographs, and insights contributed to model validation, project advancement, and provided a fundamental understanding of the future implications of this study's results. The authors also thank Yaroslav Tereshchenko for consultations at the start of the research.

---

## References

1. Landmine Monitor 2023. Available at: [https://backend.icblcmc.org/assets/reports/Landmine-Monitors/LMM2023/Downloads/Landmine-Monitor-2023\\_web.pdf](https://backend.icblcmc.org/assets/reports/Landmine-Monitors/LMM2023/Downloads/Landmine-Monitor-2023_web.pdf)
2. Two SES cadets killed in an explosion in Kharkiv region: what is known. Available at: <https://suspilne.media/kharkiv/493801-dvoe-kursantiv-dsns-zaginuli-pid-cas-vibuhu-na-harkivsini-so-vidomo>

3. Barnawi, A., Kumar, K., Kumar, N., Alzahrani, B., Almansour, A. (2024). A Deep Learning Approach for Landmines Detection Based on Airborne Magnetometry Imaging and Edge Computing. *Computer Modeling in Engineering & Sciences*, 139 (2), 2117–2137. <https://doi.org/10.32604/cmescs.2023.044184>
4. Bestagini, P., Lombardi, F., Lualdi, M., Picetti, F., Tubaro, S. (2021). Landmine Detection Using Autoencoders on Multipolarization GPR Volumetric Data. *IEEE Transactions on Geoscience and Remote Sensing*, 59 (1), 182–195. <https://doi.org/10.1109/tgrs.2020.2984951>
5. Mochurad, L., Savchyn, V., Kravchenko, O. (2023). Recognition of Explosive Devices Based on the Detectors Signal Using Machine Learning Methods. *Proceedings of the 4th International Workshop on Intelligent Information Technologies & Systems of Information Security*. <https://ceur-ws.org/Vol-3373/paper14.pdf>
6. Bai, X., Yang, Y., Wei, S., Chen, G., Li, H., Li, Y. et al. (2023). A Comprehensive Review of Conventional and Deep Learning Approaches for Ground-Penetrating Radar Detection of Raw Data. *Applied Sciences*, 13 (13), 7992. <https://doi.org/10.3390/app13137992>
7. Lameri, S., Lombardi, F., Bestagini, P., Lualdi, M., Tubaro, S. (2017). Landmine detection from GPR data using convolutional neural networks. 2017 25th European Signal Processing Conference (EUSIPCO). <https://doi.org/10.23919/eusipco.2017.8081259>
8. gprMax. Available at: <https://www.gprmax.com>
9. Srimuk, P., Boonpoonga, A., Kaemarungsi, K., Athikulwongse, K., Dentri, S. (2022). Implementation of and Experimentation with Ground-Penetrating Radar for Real-Time Automatic Detection of Buried Improvised Explosive Devices. *Sensors*, 22 (22), 8710. <https://doi.org/10.3390/s22228710>
10. Pryshchenko, O. A., Plakhtii, V., Dumin, O. M., Pochanin, G. P., Ruban, V. P., Capineri, L., Crawford, F. (2022). Implementation of an Artificial Intelligence Approach to GPR Systems for Landmine Detection. *Remote Sensing*, 14 (17), 4421. <https://doi.org/10.3390/rs14174421>
11. Kunichik, O., Tereshchenko, V. (2023). Improving the accuracy of landmine detection using data augmentation: a comprehensive study. *Artificial Intelligence*, 28 (AI.2023.28 (2)), 42–54. <https://doi.org/10.15407/jai2023.02.042>
12. Baur, J., Steinberg, G., Nikulin, A., Chiu, K., de Smet, T. S. (2020). Applying Deep Learning to Automate UAV-Based Detection of Scatterable Landmines. *Remote Sensing*, 12 (5), 859. <https://doi.org/10.3390/rs12050859>
13. Barnawi, A., Kumar, Krishan, Kumar, N., Alzahrani, B., Almansour, A. (2023). A Graph Learning Framework for Prediction of Missing Landmines Using Airborne Magnetometry in IoT Environment. <https://doi.org/10.2139/ssrn.4526746>
14. Kunichik, O., Tereshchenko, V. (2022). Analysis of modern methods of search and classification of explosive objects. *Artificial Intelligence*, 27 (AI.2022.27 (2)), 52–59. <https://doi.org/10.15407/jai2022.02.052>
15. Pahadia, H., Lu, D., Chakravarthi, B., Yang, Y. (2023). SKoPe3D: A Synthetic Dataset for Vehicle Keypoint Perception in 3D from Traffic Monitoring Cameras. 2023 IEEE 26th International Conference on Intelligent Transportation Systems (ITSC), 28, 4367–4372. <https://doi.org/10.1109/itsc57777.2023.10422667>
16. Didur, O. L., Shevchenko, M. S. (2023). MINY: yaki vykorystovuiutsia abo mozhut vykorystovuvatysia viyskamy rosiiskykh zaharbnikiv na sukhoputnomu teatri boiovykh diy. Konsultant: Hlokoza V.H. Aktualizovano – Lisnyk. Available at: [https://shron1.chtyvo.org.ua/Didur\\_Oleksandr/Miny\\_iaki\\_vykorystovuiutsia\\_abo\\_mozhut\\_vykorystovuvatysia\\_viiskamy\\_rosiiskykh\\_zaharbnikiv\\_na\\_sukhopu.pdf?PHPSESSID=7r7ecak3135fa9kap9uoqltok6](https://shron1.chtyvo.org.ua/Didur_Oleksandr/Miny_iaki_vykorystovuiutsia_abo_mozhut_vykorystovuvatysia_viiskamy_rosiiskykh_zaharbnikiv_na_sukhopu.pdf?PHPSESSID=7r7ecak3135fa9kap9uoqltok6)
17. Anti-Personnel Landmines Convention. Available at: <https://disarmament.unoda.org/anti-personnel-landmines-convention>
18. Community, B. O. (2018). Blender – a 3D modelling and rendering package, Stichting Blender Foundation, Amsterdam. Available at: <http://www.blender.org>
19. GNU Image Manipulation Program. Available at: <https://www.gimp.org/about>
20. Prusa Research. Available at: [https://www.prusa3d.com/page/about-us\\_77](https://www.prusa3d.com/page/about-us_77)
21. PMN AP MINE (Historical Prop) by mussy is licensed under the Creative Commons – Attribution – Non-Commercial – No Derivatives license. Available at: <https://www.thingiverse.com/thing:3157971>
22. PMN-2. by \_-HB-\_ is licensed under the Creative Commons – Attribution license. Available at: <https://www.thingiverse.com/thing:5777217>
23. PMN-2 Landmine. Available at: <https://mmf.io/o/98395>
24. OZM-72 Anti-Personnel Mine Gameready Lowpoly. Available at: <https://sketchfab.com/3d-models/ozm-72-anti-personnel-mine-gameready-lowpoly-9226037a15ab47bd9fb08ed434ea1ae8>
25. MON-50. MOH-50. Soviet claymore shaped AP-mine. Available at: <https://sketchfab.com/3d-models/mon-50-50-soviet-claymore-shaped-ap-mine-5a5da292827f41278df15e4fcee85807>
26. PFM-1 AP MINE (Historical Prop). Available at: <https://www.thingiverse.com/thing:3660586>
27. Redmon, J., Divvala, S., Girshick, R., Farhadi, A. (2016). You Only Look Once: Unified, Real-Time Object Detection. 2016 IEEE Conference on Computer Vision and Pattern Recognition (CVPR). <https://doi.org/10.1109/cvpr.2016.91>
28. Jocher, G., Qiu, J., Chaurasia, A. (2023). Ultralytics YOLO (Version 8.0.0) [Computer software]. Available at: <https://github.com/ultralytics/ultralytics>
29. Reis, D., Kupec, J., Hong, J., Daoudi, A. (2023). Real-Time Flying Object Detection with YOLOv8. arXiv. Available at: <https://doi.org/10.48550/arXiv.2305.09972>

30. Waite, J. R., Feng, J., Tavassoli, R., Harris, L., Tan, S. Y., Chakraborty, S., Sarkar, S. (2023). Active shooter detection and robust tracking utilizing supplemental synthetic data. arXiv. <https://doi.org/10.48550/arXiv.2309.03381>
31. Lou, H., Liu, H., Bi, L., Liu, L., Guo, J., Gu, J. (2023). Bd-Yolo: Detection Algorithm for High-Resolution Remote Sensing Images. <https://doi.org/10.2139/ssrn.4542996>
32. Kang, M., Ting, C.-M., Ting, F. F., Phan, R. C.-W. (2023). RCS-YOLO: A Fast and High-Accuracy Object Detector for Brain Tumor Detection. *Medical Image Computing and Computer Assisted Intervention – MICCAI 2023*, 600–610. [https://doi.org/10.1007/978-3-031-43901-8\\_57](https://doi.org/10.1007/978-3-031-43901-8_57)
33. Ang, G. J. N., Goil, A. K., Chan, H., Lew, J. J., Lee, X. C., Mustaff, R. B. A. et al. (2023). A Novel real-time arrhythmia detection model using YOLOv8. arXiv. <https://doi.org/10.48550/arXiv.2305.16727>
34. Agarwal, V., Pichappa, A. G., Ramisetty, M., Murugan, B., Rajagopal, M. K. (2023). Suspicious Vehicle Detection Using Licence Plate Detection And Facial Feature Recognition. arXiv. <https://doi.org/10.48550/arXiv.2304.14507>
35. Zhou, F., Deng, H., Xu, Q., Lan, X. (2023). CNTR-YOLO: Improved YOLOv5 Based on ConvNext and Transformer for Aircraft Detection in Remote Sensing Images. *Electronics*, 12 (12), 2671. <https://doi.org/10.3390/electronics12122671>
36. Rublee, E., Rabaud, V., Konolige, K., Bradski, G. (2011). ORB: An efficient alternative to SIFT or SURF. 2011 International Conference on Computer Vision. <https://doi.org/10.1109/iccv.2011.6126544>
37. Alcantarilla, P., Nuevo, J., Bartoli, A. (2013). Fast Explicit Diffusion for Accelerated Features in Nonlinear Scale Spaces. *Proceedings of the British Machine Vision Conference 2013*, 13.1-13.11. Available at: <https://projet.liris.cnrs.fr/imagine/pub/proceedings/BMVC-2013/Papers/paper0013/paper0013.pdf>
38. Tan, M., Pang, R., Le, Q. V. (2020). EfficientDet: Scalable and Efficient Object Detection. 2020 IEEE/CVF Conference on Computer Vision and Pattern Recognition (CVPR). <https://doi.org/10.1109/cvpr42600.2020.01079>
39. Carion, N., Massa, F., Synnaeve, G., Usunier, N., Kirillov, A., Zagoruyko, S. (2020). End-to-End Object Detection with Transformers. *Computer Vision – ECCV 2020*, 213–229. [https://doi.org/10.1007/978-3-030-58452-8\\_13](https://doi.org/10.1007/978-3-030-58452-8_13)
40. Zhu, X., Su, W., Lu, L., Li, B., Wang, X., Dai, J. (2020). Deformable DETR: Deformable Transformers for End-to-End Object Detection. arXiv. <https://doi.org/10.48550/arXiv.2010.04159>